Chapter 1: Introduction

1.1 General introduction

A fundamental tenet of metamorphic petrology is the assumption that rocks attain and maintain chemical equilibrium at elevated temperatures. Rocks undergo chemical reactions during the changing pressure-temperature conditions experienced in orogenic processes. These chemical reactions involve dissolution of reactants, mass transfer through the rock medium and the growth of new product minerals. The resulting mineral assemblages equilibrate along an evolutionary pressure-temperature (*P-T*) path as long as fluid or melt is present to facilitate mass transfer, and reaction is arrested or retarded when melt or fluid is absent (White and Powell, 2002; Powell et al., 2005). As a result, the assemblage observed in the rock today can be used to infer conditions at which fluid or melt was lost (White and Powell, 2002; Powell et al., 2005). This equilibrium model of metamorphism has allowed the application of equilibrium thermodynamics to the forward and inverse modelling of metamorphic textures (e.g., White et al., 2002; Boger et al., 2003; White et al., 2003; Johnson et al., 2003; Kelsey et al., 2003a; Kelsey et al., 2003b; Johnson et al., 2004; Zeh et al., 2004; Baldwin et al., 2005; White et al., 2005; Hollis et al., 2006; Diener et al., 2007; Halpin et al., 2007). Much of our understanding of tectonics and orogenesis is founded on the information derived from metamorphic rocks in this way.

An assemblage is considered to be in equilibrium if it has the lowest Gibbs free energy (Prigogine and Defay, 1954; Denbigh, 1971; Spear, 1993). With changing pressure and temperature during orogenesis or contact metamorphism, mineral assemblages, modal proportions and compositions will change to attain a new lowest Gibbs free energy equilibrium configuration. At chemical equilibrium there are no gradients in chemical potentials for any components in the volume considered. Equilibration is a function of complex interdependent relationships between evolving bulk composition, grain size, temperature, heating and/or cooling rate (e.g., Carlson, 2002; Marmo et al., 2002; White et al., 2002; White et al., 2004; Johnson et al., 2004; Evans et al., 2004). Whether a rock is in equilibrium or not, is largely a question of the scale considered (Stüwe, 1997; Carlson, 2002; White et al., 2008). Equilibration can be seen as a continuum ranging from complete equilibration for all components at scales of metres to tens of metres, to partial equilibration on the scale of microns to millimetres and, finally, complete disequilibrium in extreme strain rate environments realised in large meteorite impact craters.

The recognition of scales of equilibration has largely been driven by technological advances in analytical techniques allowing zonation of components on ever-decreasing scales to be resolved. Analytical precision has, in turn, driven increasing refinements to modelling metamorphic systems. Powell and Holland (1988, 1994) devised a software tool, THERMOCALC, which allowed the calculation of P and T conditions of formation for a metamorphic assemblage, based on the measured compositions of phases (avPT), predicated on the equilibrium model of metamorphism. With gradual improvements in thermodynamic data sets of mineral end-members (Holland and Powell, 1996; Berman, 1988; Holland and Powell, 1998; upgrade November 2003) and a-x relationships for minerals and, especially appropriate for granulite-facies rocks, silicate liquid and fluid (e.g., Powell, 1987; Holland and Powell, 1992; Powell and Holland, 1993; Holland and Powell, 1996; Powell and Holland, 1999; Dale et al., 2000; White et al., 2000; Holland and Powell, 2001; White et al., 2001; Holland and Powell, 2003; Dale et al., 2005; Diener et al., 2007), it became possible to model the evolution of assemblages in P-T space through constant composition phase diagrams or pseudosections (Powell and Holland, 1998).

The difficulty in determining original phase compositions required for conventional thermobarometry, and large uncertainties of attendant P-T estimates, has made pseudosection thermobarometry the preferred technique for reconstructing the metamorphic evolution of a rock. In pseudosections, the boundaries between fields of alternative mineral assemblages constrain P-T estimates for formation of an observed assemblage, not uncertainties as in conventional thermobarometers (Powell and Holland, 2008). Pseudosections also allow reconstruction of the P-T path through comparison of inclusion and textural relationships in an observed assemblage with corresponding mineral modes and compositions in assemblages that could have developed given a range of potential P-T conditions in the pseudosection. Currently, it is possible to model bulk compositions in MnNCKFMASHTO (MnO-Na_2O-CaO-K_2O-FeO-MgO-Al_2O_3-SiO_2-H_2O-TiO_2-Fe_2O_3). Ongoing improvements in the thermodynamic mineral data set and *a-x* relationships coupled with continued advance in analytical methods ensure expansion of modelling capacity into larger model chemical systems (e.g., including Zn). New capacity in THERMOCALC allows modelling of chemical potential relationships governing the spatial organization of phases within an equilibration volume (e.g., White et al., 2008). It is now possible to model complex reaction textures (e.g., coronas) in terms of evolving chemical potentials through open-system metasomatic exchange of selected components with the external system.

This study is primarily concerned with an investigation of reaction dynamics and processes across the equilibration continuum. The range of scales of equilibration across the continuum is schematically demonstrated in Figure 1.1. During peak, anatectic granulite facies metamorphic events, chemical potential gradients may be eliminated for all major components in equilibration volumes on the scale of metres to tens of metres (Figure 1.1a). This is typically the scale of equilibration volume considered when modelling peak metamorphism of granulites prior to melt loss (White et al., 2008). Under peak granulite conditions, complete equilibration is attained through melt- and/or fluid-assisted diffusion with comparatively long reaction durations. The coarse-grained evolution of a rock will cease when melt is lost from the equilibration volume or the solidus is crossed on the retrograde path with cooling (White and Powell, 2002). Equilibration following peak conditions becomes a more complex process and requires consideration of equilibration volumes an order of magnitude smaller on the scale of microns to centimetres.

In the post-peak, melt-depleted restite, in the absence of deformation and/or low melt volumes and/or rapidly changing P and T, reaction becomes diffusion-controlled. Here, length-scales of diffusion for major components are decoupled, the bulk composition is partitioned and segregated reaction products develop (Figure 1.1b), typically as a corona (Fisher, 1977; Joesten, 1977; Mongkoltip and Ashworth, 1983; Foster, 1986; Grant, 1988; Johnson and Carlson, 1990; Carlson and Johnson, 1991; Ashworth and Birdi, 1990; Ashworth et al., 1992; Ashworth and Sheplev, 1997; Markl et al., 1998; Ashworth et al., 1998). At this scale, chemical potential gradients may be eliminated for mobile components, but remain entrenched for the more slowly diffusing components. The attainment of equilibrium for some components and not for others is described as partial equilibrium (Carlson, 2002). The length scales of diffusion for rare earth elements are now known to be much smaller than major elements (e.g., Spear and Kohn, 1996; Pyle and Spear, 1999; Carlson, 2002; Clarke et al., 2007), revealing information about processes and the role of accessory minerals in which they occur in abundance (Kelsey et al., 2008; Clarke et al., 2007).

Partial equilibration of post-peak supra-solidus assemblages may occur either progressively or non-progressively (e.g., White et al., 2009). In progressive post-peak metamorphism, there is a continuous change in the stable post-peak equilibrium assemblage as the *P-T* path tracks across a phase field in a pseudosection and the modes (abundances) of minerals shift accordingly (White et al., 2009). In progressive corona development, no crossing of a univariant reaction line is required. The reactants may remain part of the stable equilibrium assemblage, however, the modes of the minerals shift according to the *P-T* trajectory through the phase field. Reaction may go to completion as the melt is consumed at the solidus. Non-progressive corona growth occurs in polymetamorphic terranes, under *P-T* conditions that are markedly different from that of the peak assemblage, with potential assemblages that lie between the different *P-T* conditions in the pseudosection undeveloped (White et al., 2009). In non-progressive metamorphism, the peak assemblage is preserved at the solidus and no further reaction occurs until the rock is heated once more under different pressures and temperatures in excess of the dry solidus for the restitic composition (White and Powell, 2002).

An extreme metamorphic scenario is that in which equilibrium is unattainable at any measureable scale for any component. The only process capable of inducing disequilibrium to such an extent is bolide (meteorite) impact, which releases immense energy into the crust as the kinetic energy of the bolide is transformed instantaneously into a shock wave that radiates outwards into the target rocks. Shock pressures in the target crust may range from 2 to 100 GPa with associated instantaneous shock heating to temperatures as high as 2000 °C in the most highly shocked crust closest to the point of impact (Figure 1.1c). The shock wave compresses the target rocks at pressures above the Hugoniot elastic limit, inducing irreversible structural and phase changes in target minerals, termed shock-metamorphic effects (see review in French, 1998), which are heterogeneously distributed throughout the target rock. Shock metamorphic effects in quartz might include planar deformation lamellae (< 5µm) at 10 to 35 GPa (Figure 1.1c) and shock-induced isotropisation of entire mineral grains at shock pressures > 35 GPa (French, 1998). Whole-mineral melts, typically of feldspar and micas, occur as components of melt breccias at shock pressures > 45 GPa (Ostertag, 1983). The extremely heterogeneous distribution of shock effects throughout the target rock negates the application of an equilibrium model of metamorphism.

Within a fraction of a second to, at most, seconds after impact, adiabatic decay of the shock wave following non-adiabatic loading during impact, leads to post-shock heating of the target rocks (Raikes and Ahrens, 1979). This post-shock heating is proportional to the peak shock pressure and can exceed 1000 °C in highly shocked rocks (e.g., Stöffler, 1972). In large impacts, shock effects and the subsequent post-shock heating may affect mid- and lower-crustal levels that remain buried after the impact. Under such conditions the cumulative effect of shock heating and residual heat from the pre-impact crustal geotherm is capable of inducing static metamorphism in the crust, leading to annealing and partial equilibration of shock-induced deformation features and any pre-impact metamorphic assemblages (Gibson and Reimold, 2005).

The *P-T* fields for conventional and shock metamorphism (Figure 1.1) are so vastly different, most treatises on metamorphism do not even consider them together. One of the few geological settings where it is possible to investigate the nature and complexity of equilibration across this continuum is the Vredefort Dome, South Africa. This metamorphic environment presents the closest possible natural analogue to laboratory conditions preserving diagnostic textural and compositional intricacies across the equilibration continuum.

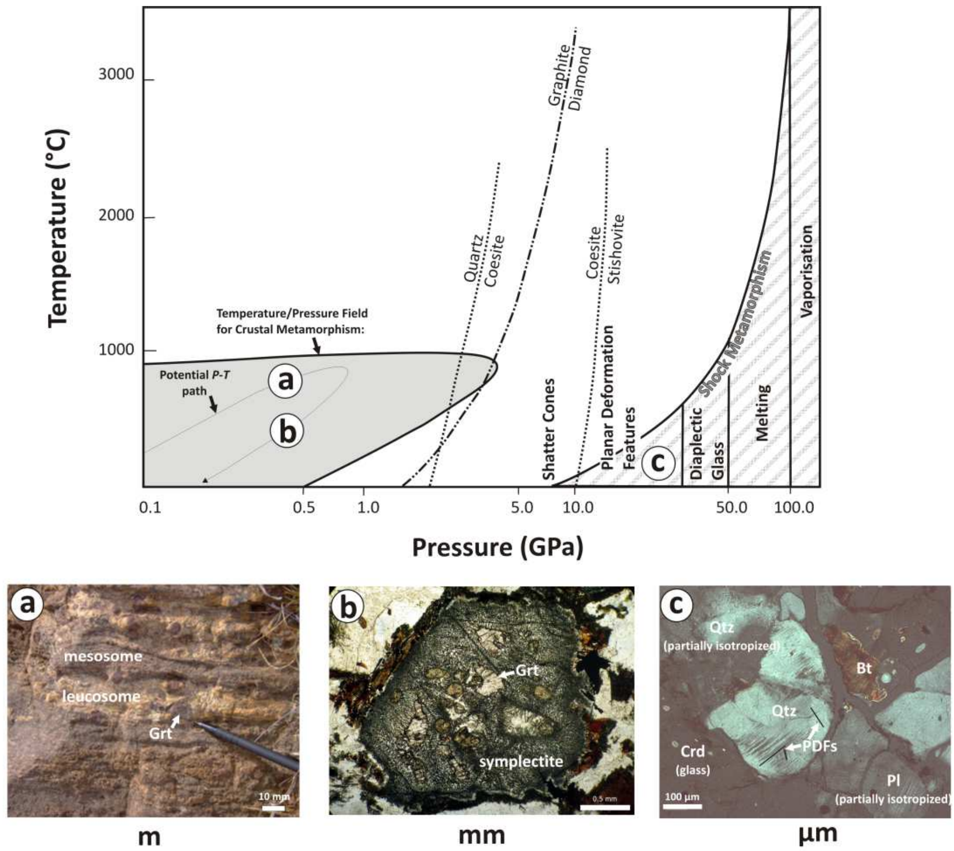

	Regional/Contact Metamorphism:		Shock Metamorphism:
Strain rate:	10^{-3} s^{-1} to 10^{-6} s^{-1}		10^{6} s^{-1} to 10^{9} s^{-1}
Temperature:	Generally < 1000 °C		typically up to 3000 °C
Duration:	10^{5} - 10^{7} yr		µs - minutes
Bulk Composition:	Melt/fluid present	Melt-depleted restite	Any
Equilibrium:	Complete for all components	Partial - complete for rapidly diffusing components	Disequilibrium at scales < 10 µm

Equilibration scale

***Figure 1.1:** A demonstration of the equilibration continuum from (a) complete equilibration in melt-rich granulite events, to (b) partial equilibration in melt-depleted restites to form coronas, and finally (c) complete disequilibrium with extreme strain rates and highly localised shock deformation effects in shock metamorphism. P-T graph modified from French (1998).*

1.2 Geology of the Vredefort Dome

The Vredefort Dome is a 90-km-wide impact-induced central uplift structure formed by rebound of the shocked basement beneath a giant, 2.02 Ga, complex crater that was originally 250 - 300 km in diameter (Figure 1.2). Complex craters form during large impact events, in which the energy released into the target rocks is sufficient to ensure sub-crater rheology approaches a Bingham fluid rather than competent or unconsolidated rock (Collins et al., 2000). Under these conditions, the sub-crater rocks rise to form a central uplift during late-stage modification of the original transient crater (French, 1998), while rocks around the periphery of the crater collapse to form a terraced structure. The Theophilus lunar impact structure is an excellent example of a pristine complex crater (Figure 1.3) with a clear central uplift and terraced inner crater rim.

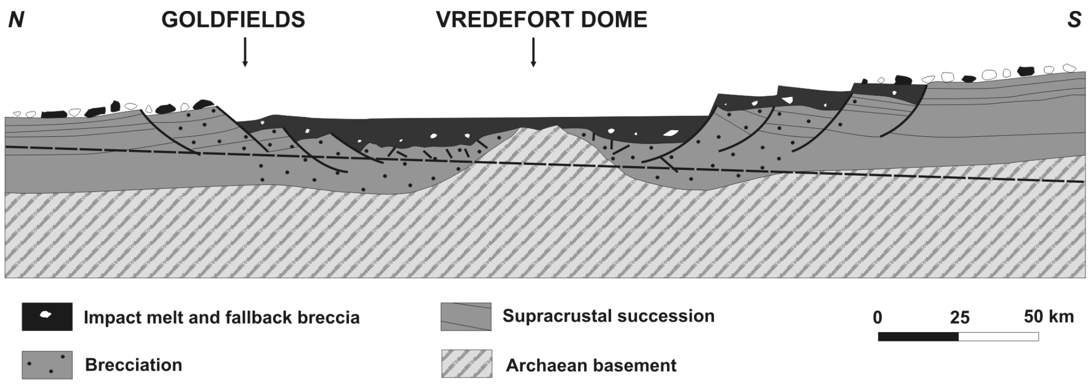

Figure 1.2: Schematic cross-section through the Vredefort complex crater formed after impact at 2.02 Ga, comprising a central uplift (Vredefort Dome) and terraced crater walls. The dashed line represents the current level of erosion (modified after Gibson and Reimold, 2001).

The Dome is located ~ 120 km south of Johannesburg and is surrounded by a 50 - 70 km wide synclinorium comprising the gold-bearing strata of the Witwatersrand Supergroup, and the Ventersdorp and Transvaal Supergroups (Figure 1.4). Erosion of between 5 and 10 km of overlying rocks (McCarthy et al., 1990) has exposed an ~ 40 km wide core of amphibolite to granulite facies Meso-Archaean gneisses (Archaean Basement Complex, Figure 1.5). Surrounding the basement rocks, is a 20 to 25 km wide collar of Late Archaean to Palaeoproterozoic supracrustal strata (Dominion Group and Witwatersrand, Ventersdorp and Transvaal Supergroups) that were deposited unconformably on the basement commencing at 3074 ± 6 Ma (Armstrong et al., 1991). The southern and central parts of the Dome are obscured beneath Palaeozoic Karoo Supergroup sediments and dolerite sills (Figure 1.5). In the southeast of the Dome, a sequence of greenschist to amphibolite facies mafic and ultramafic schists of komatiitic and komatiitic basalt composition is exposed south of a Meso-Archaean shear zone (Broodkop shear zone; Lana et al., 2006).

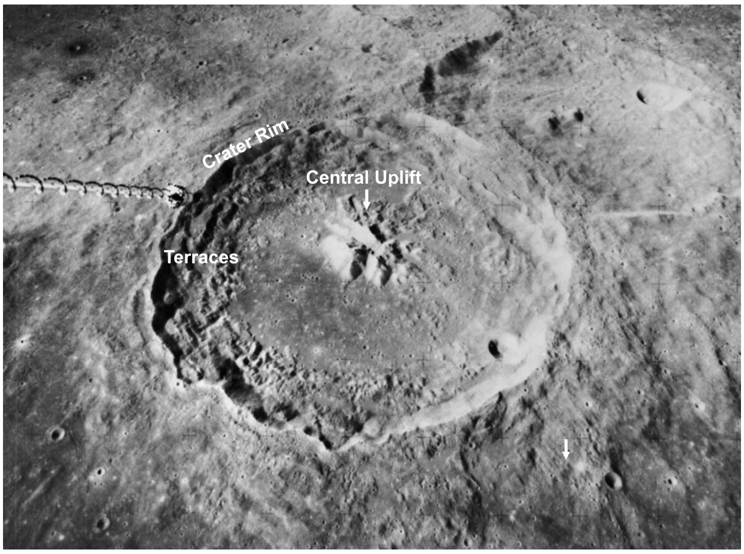

Figure 1.3: The Theophilus lunar impact structure is a complex crater, with a clear central uplift and terraced inner crater rim. The structure is 100 km in diameter. Image courtesy of NASA.

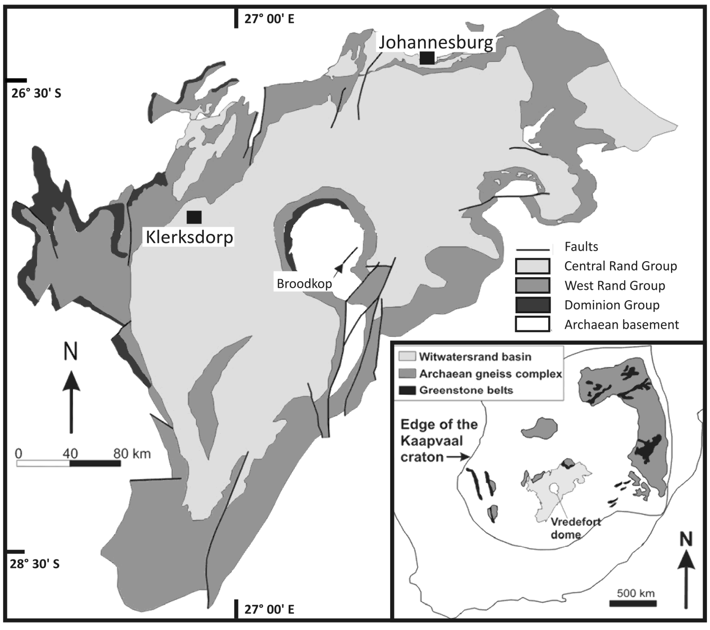

Figure 1.4: Simplified geological map showing the location of the Witwatersrand basin and Vredefort Dome (after Lana et al., 2006).

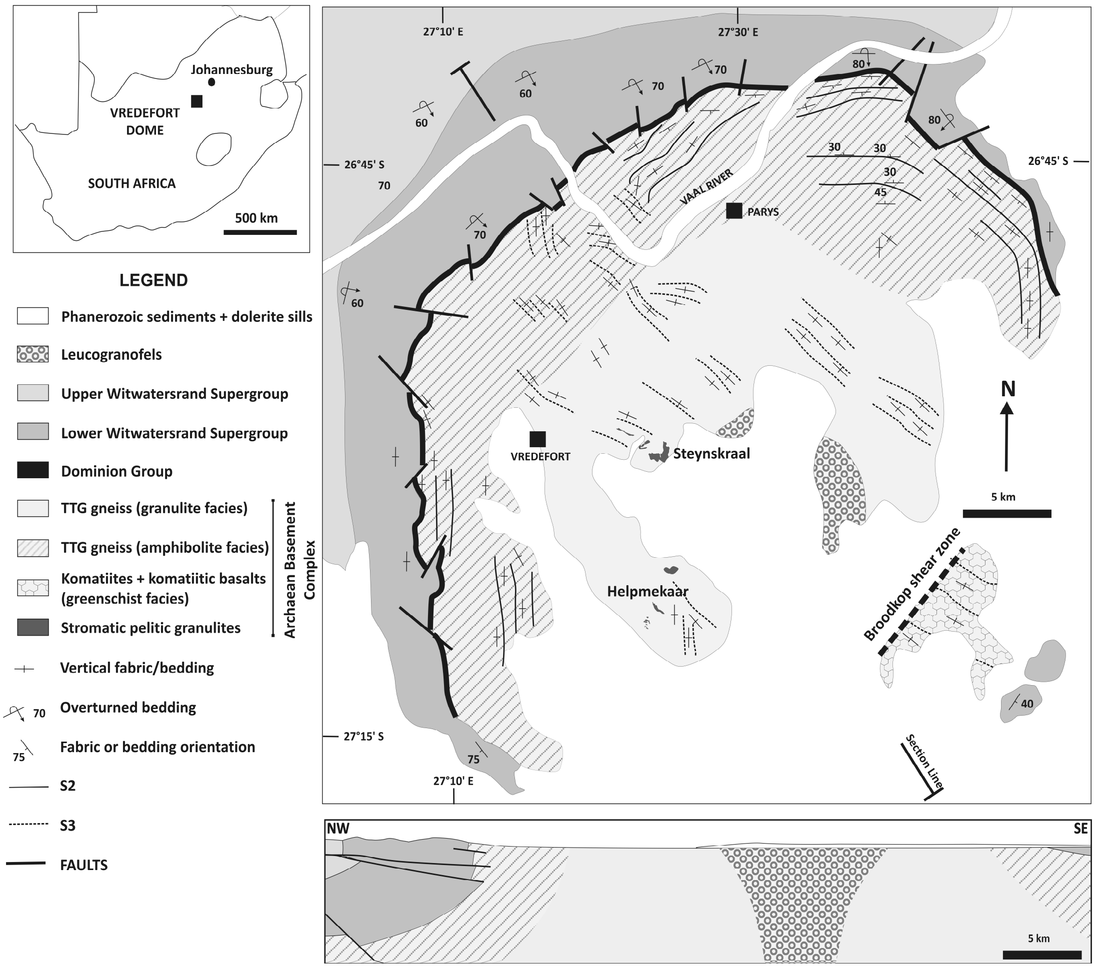

Figure 1.5: Geological map and cross-section of the Vredefort Dome indicating main lithologies and distribution of pelitic greenstone remnants in the Archaean Basement Complex in the core of the Dome (modified after Armstrong et al., 2006).

Shock metamorphic effects developed in the Vredefort Dome include shatter cones, planar deformation features (PDFs) in quartz and feldspar, pseudotachylitic breccias, and impact melt (Gibson and Reimold, 2008). Shock metamorphic effects show a broad concentric distribution (Figure 1.6) increasing in intensity toward the centre of the Dome, but exhibit marked heterogeneity at both the outcrop- and thin section scale (Gibson and Reimold, 2005). Gibson and Reimold (2005) produced a detailed map of shock distribution throughout the Dome based on the occurrence of shock effects observed in minerals, predicting maximum pressures of 35 – 40 GPa toward the centre of the Dome (Figure 1.6). Numerical modelling of the Vredefort structure (Ivanov, 2005) constrains peak shock pressures approaching 60 GPa in the centre of the Dome (Figure 1.7a), 15 GPa in excess of shock pressures inferred from shock effects in minerals by Gibson and Reimold (2005). A component of this study aims to evaluate the apparent discrepancy between numerical estimates of shock pressures and those deduced from shock effects in minerals observed petrographically.

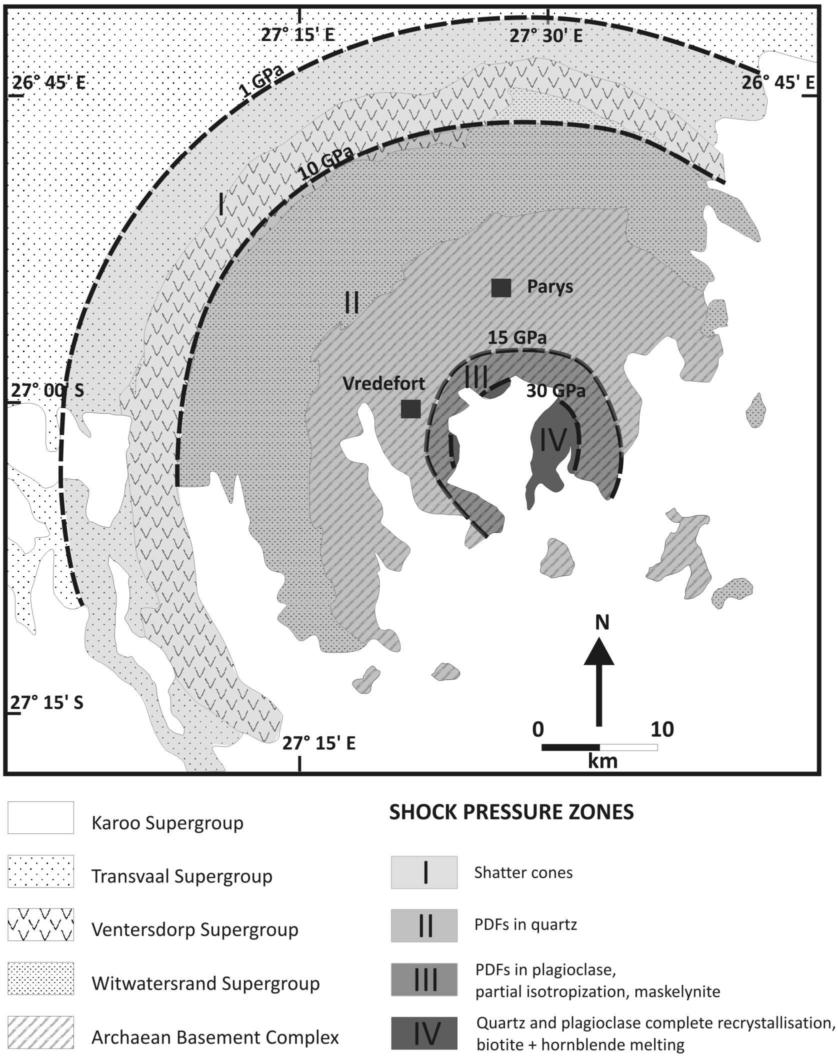

Figure 1.6: Shock pressure distribution throughout the Vredefort Dome based on observed mineral and rock textures (modified after Gibson and Reimold, 2005).

Among the effects attributed to the Vredefort impact event is a strongly variable thermal overprint caused by decay of the shock pressure following non-adiabatic shock-loading, which increases in intensity radially towards the centre of the Dome (Gibson et al., 1998; Gibson, 2002; Ivanov, 2005; Figure 1.7).

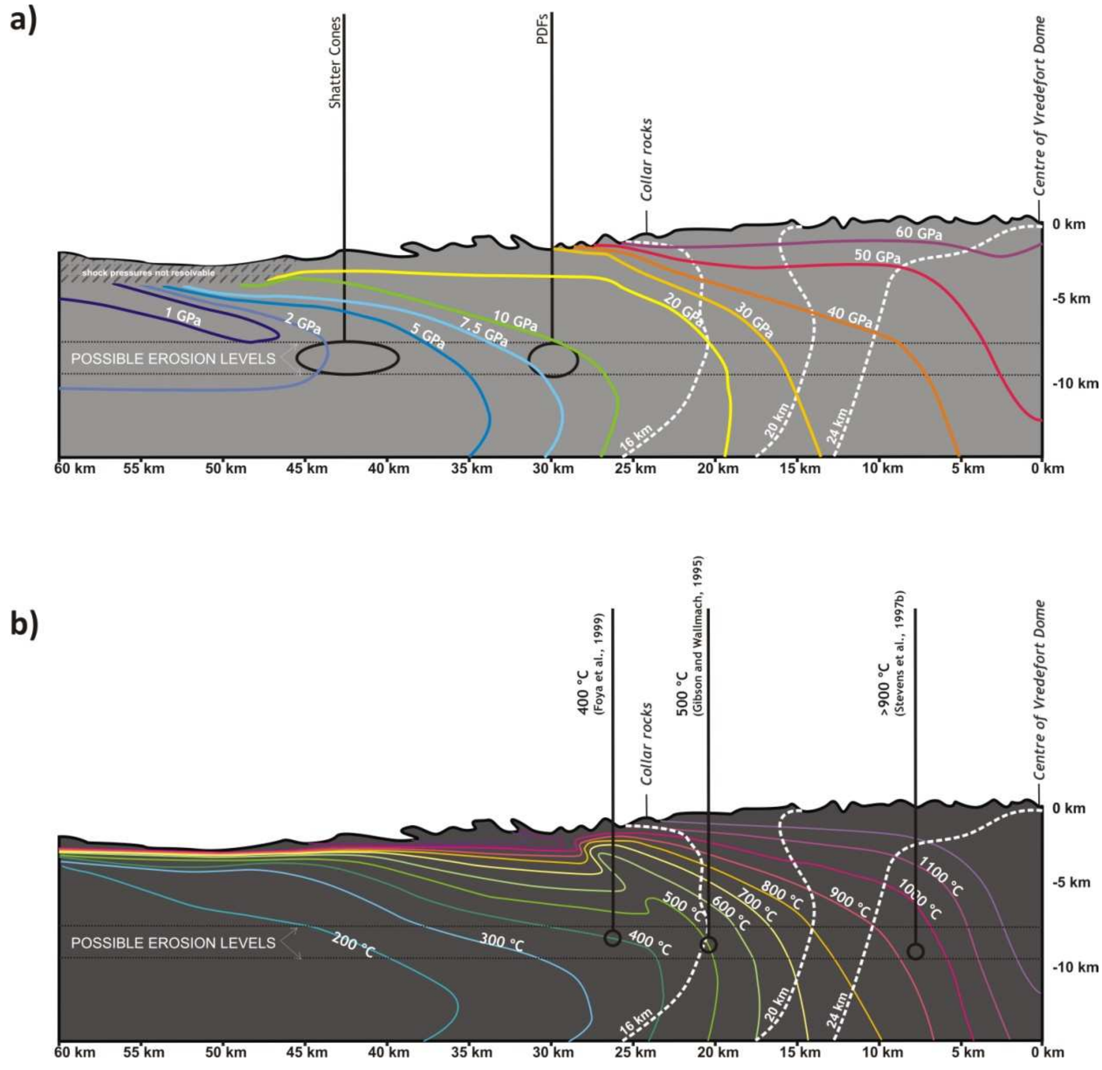

Figure 1.7: Numerical models for (a) shock pressure and (b) post-shock temperature distribution throughout the Vredefort Dome (modified after Ivanov, 2005). Coloured contour lines represent shock pressure contours in (a) and post-shock isotherms in (b). Dotted white isolines represent initial depths of burial prior to impact. Black circles in (a) indicate occurrence of diagnostic shock effects and in (b) indicate points of agreement between observed temperature estimates from thermobarometry (e.g., Stevens et al., 1997b) and the numerical model. Thermobarometric estimates have been used to constrain the boundary conditions and, as such, the numerical model is limited by the accuracy of these initial estimates and post-impact temperatures may well have been higher closer to the centre of the Dome.

Figure 1.7b demonstrates the post-shock temperature distribution profile in the core of the Vredefort Dome generated from numerical modelling (Ivanov, 2005). Post-shock temperature varies as a function of both shock pressure - which increases radially towards the centre of the Dome (Gibson and Reimold, 2005) - and the pre-impact geotherm, which according to Gibson and Jones (2002), was 20 °C/km immediately prior to impact. Thus, the radially-inward increase in temperature from < 300 °C to > 1000 °C reflects both the exponential increase in shock pressure and increased level of doming-induced exhumation towards the centre of the Dome.

Ivanov (2005) calculated that the rocks at the present level of exposure were sufficiently insulated to have remained hot for several hundred thousand years and, consequently, that the rocks were capable of re-equilibrating under new metamorphic conditions of 2 - 3 kbar and 300 - 1000 °C. Earlier studies by Gibson and Wallmach (1995) and Gibson et al. (1998) have provided broad confirmation of the increase in temperature toward the centre of the Dome. Gibson (2002) also described textures invoking exceptional temperatures in excess of 1000 °C in the centre of the Dome. The considerable uncertainties in methods employed for *P-T* determination and a range of other *P* and *T* estimates obtained from the same rocks by other authors (Schreyer and Abraham, 1978; Stevens et al., 1997b; Perchuk et al., 2002) necessitates a reappraisal. In this study, rocks from the Archaean Basement Complex are revisited to further refine post-shock conditions.

1.3 Geology of the Archaean Basement Complex

The Archaean Basement Complex exposed in the core of the Vredefort Dome includes metapelitic, metagreywacke, metamafic and lesser meta-ironstone xenoliths enclosed within 3120 - 3100 Ma tonalitic and trondhjemitic gneisses (Lana et al., 2004; Armstrong et al., 2006). Several NW-SE trending pelitic and mafic granulites occur on the farms Steynskraal and Jagers Vrede, between 5 and 8 km to the northwest of the centre of the Dome (hereafter referred to as the Steynskraal granulites) and on the farm Helpmekaar to the southwest of the centre of the Dome (Figure 1.5). The radial array of discontinuous granulite outcrops on the Steynskraal and Jagers Vrede farms is hereafter referred to as the Steynskraal traverse (Figure 1.5). The granulites form part of an Archaean volcano-sedimentary sequence, occurring as discontinuous, elongate rafts within intrusive tonalite-trondhjemite-granodiorite gneisses (Stepto, 1990; Flowers et al., 2003; Lana et al., 2004).

The metasedimentary granulites comprise stromatic and locally massive Grt-Bt-Crd/Opx (abbreviations after Kretz, 1983) restites and range from pelitic to greywacke bulk compositions (Stevens et al., 1997b; Gibson, 2002). Stromatic pelitic granulites are characterized by Grt-Bt-Crd mesosomes alternating with thinner Grt-Pl-Kfs leucosomes. Less aluminous and potassic greywacke bulk compositions comprise Grt-Bt-Opx mesosomes with Grt-Pl±Kfs leucosomes. Less commonly, granulites appear massive, with no discrete leucosomes and are markedly restitic, consistent with almost complete melt loss. Overprinting the coarse-grained assemblages are shock metamorphic effects associated with the 2.02 Ga impact, including pseudotachylitic breccias; planar deformation features in quartz and plagioclase; and planar fractures in feldspar and quartz (e.g., Schreyer and Abraham, 1978; Stevens et al., 1997b; Gibson and Reimold, 2005). Corona textures comprising complex multi-layered product symplectites and bands are developed around garnet (Schreyer and Abraham, 1978; Stevens et al., 1997b; Gibson, 2002).

Lana et al. (2004) and Armstrong et al. (2006) identified three magmatic TTG suites in the Archaean Basement Complex, each associated with a specific deformation event. The oldest, biotite-rich, trondhjemitic gneiss is found as xenoliths within the main trondhjemitic gneiss that occurs as sparse, scattered outcrops in the northeast of the Dome. The xenoliths retain evidence of an early S1 fabric that has been largely transposed by D2 elsewhere in the Dome (Lana et al., 2003a). Both the xenoliths and the host trondhjemitic gneiss give ages of 3113.8 ± 4.8 Ma (Armstrong et al., 2006). These rocks have been intruded by a younger, 3105 ± 5 Ma, porphyritic granite (Armstrong et al., 2006), exposed in the western sector of the core of the Dome. Lana et al. (2004) suggested that intrusion of the granodiorite occurred during the D2 event and was associated with pervasive development of a subhorizontal S2 fabric throughout the TTG gneisses. The D2 event was followed by the intrusion of a younger suite of granitic to granodioritic bodies emplaced at 3092 ± 6.2 Ma (Armstrong et al., 2006) during a northeast-southwest compressional event under intermediate-P, high-T metamorphic conditions. The D3 event was characterised by the development of a northwest-trending, subvertical peak-metamorphic S3 fabric. D3 was intimately linked to both tectonic and magmatic crustal thickening with high-grade peak metamorphism during the northeast-southwest compressional event (Stevens et al., 1997b; Lana et al., 2003a). Although the TTG rocks and the syntectonic granitoids and leucosomes were emplaced during distinct deformation events, the differences in age between these rocks are within uncertainty (Armstrong et al., 2006). Essentially indistinguishable age data and geochemical evidence (Lana et al., 2004) suggests that the TTG suite and the granitic leucosomes and granitoids are part of a single, continuous, magmatic episode in which the leucosomes represent more fractionated melts from the original trondhjemitic parent magma (Armstrong et al., 2006).

Crustal thickening and accretion of the Vredefort rocks onto the Kaapvaal craton at 3100 – 3080 Ma occurs only 10 – 25 Myr prior to the outpouring of the 3074 ± 6 Ma (Armstrong et al., 1991) Dominion Group lavas onto upper amphibolite facies basement, implying extremely rapid exhumation rates. Given the petrological evidence at the time which suggested an anticlockwise *P-T* path (Stevens et al., 1997b), Lana et al. (2006) proposed rapid extensional unroofing and collapse of the thickened crust occurred during D4 at 3068 ± 6 Ma along a subhorizontal to gently northwest-dipping shear zone now preserved in the southeastern sector of the Dome (Broodkop shear zone; Lana et al., 2006; Armstrong et al., 2006). The D4 event has been dated from aplite dykes cross-cutting the D4 shear zone (Armstrong et al., 2006). This led to the structural juxtaposition of low-grade greenschist facies komatiites and komatiitic basalts in the southeast of the Dome with high-grade, granulite facies gneisses to the northwest. Lana et al. (2006) linked this extension to the rifting associated with extrusion of the 3074 ± 6 Ma Dominion Group lavas.

1.4 Metamorphic evolution of the Vredefort Dome

A comprehensive review of metamorphism in the collar rocks of the Dome is given in Gibson and Reimold (2008). This study focuses on the Archaean Basement Complex in the core of the Dome (Figure 1.5). Based on numerical modelling (Ivanov, 2005), these rocks appear to have resided in the mid to lower crust (16 - 27 km) immediately prior to the impact. Exhumation during central uplift formation has exposed an oblique section through the crust, preserving granulite facies gneisses in the centre, and originally less deeply buried upper amphibolite facies rocks further from the centre. The Archaean Basement Complex comprises mainly TTG gneisses. The high-variance assemblages typical of TTG gneisses are not particularly informative with regard to metamorphic conditions. However, the rare pelitic, ironstone and mafic granulite xenoliths are far more sensitive to changes in metamorphic conditions. These have been studied by a variety of authors (Willemse, 1937; Schreyer and Abraham, 1978; Schreyer, 1983; Stepto 1979, 1990; Stevens et al., 1997b; Gibson et al., 1998; Gibson, 2002; Perchuk et al., 2002) who have come to contrasting conclusions regarding the origin of textures.

Interpretations of the metamorphic history of the pelitic xenoliths of the Archaean Basement Complex have reflected the evolving debate and eventual consensus regarding the origin of the Dome, i.e., endogenic vs. exogenic mechanisms for Dome formation. Endogenic models for Vredefort Dome formation invoke a magmatic heat source at the centre of the Dome, with anomalous deformation features (shatter cones, pseudotachylitic breccias, etc.) attributed to explosive magmatic processes (e.g., Nicolaysen and Ferguson, 1990). This interpretation appeared to accommodate a metamorphic field gradient showing a radial increase in temperature towards the centre of the Dome, from greenschist and mid-amphibolite facies ‘hornfelsic’ Witwatersrand strata in the collar to granulite facies cordierite-orthopyroxene symplectites after garnet in the core of the Dome (Schreyer and Abraham, 1978; Schreyer, 1983). One of the basic premises of Schreyer’s (1983) endogenic model was an apparent crosscutting relationship between the pseudotachylitic breccias and the Crd-Opx symplectites, i.e., symplectite between garnet and matrix phases appears truncated by younger pseudotachylitic breccias and symplectite is undeveloped between garnet and the pseudotachylitic breccia matrix. Accordingly, pseudotachylitic breccias were inferred by Schreyer (1983) to reflect a late-stage, high-strain-rate event during a static granulite event generated by a local magma diapir. A number of alkali granite bodies in the collar of the Dome were interpreted to be surface expressions of a larger, deeper pluton to which the static granulite overprint was attributed (Hall and Molengraaff, 1925; Nicolaysen, 1990). Schreyer & Abraham (1978) used experimental data from Hensen & Green (1971, 1972, 1973) to infer conditions of Crd-Opx symplectite formation of 5 kbar and 700 °C.

As conclusive evidence of an impact origin for the Vredefort Dome accumulated, i.e., discovery of coesite and stishovite (Martini, 1978) and a meteoritic component in the dykes of Vredefort Granophyre (Koeberl et al., 1996), the granulites in Steynskraal were revisited in an attempt to reconcile the metamorphic textures with the impact event (Stevens et al., 1997b; Gibson et al., 1998; Gibson, 2002). These workers identified an unusual polymetamorphic history involving three discrete events, each reflecting equilibration at a different scale.

1.4.1 M_1: peak anatectic event (3.1 Ga)

The restitic, coarse-grained assemblages observed in the Steynskraal metapelites of Grt-Crd-Bt-Opx-Qtz-Pl-Kfs were interpreted by Stevens et al. (1997b) as products of near-complete melt loss during a peak anatectic event (M_1). As is typical of peak granulite events, equilibrium is attained at the outcrop- or metre-scale. Stevens et al. (1997b) constrained temperatures during M_1 based on the stability of coexisting biotite and H_2O-undersaturated melt (Stevens et al., 1997a). Accordingly, biotite-absent Grt-Opx/Crd-Qtz-Pl-Kfs restites indicated temperatures in excess of the upper stability limit of biotite, i.e., > 920 °C (Stevens et al., 1997a). Peak pressures of 5 - 5.5 kbar were determined using the Hensen and Green (1973) conventional geobarometer based on coexisting garnet, cordierite, orthopyroxene and quartz (Stevens et al., 1997b). Stevens et al. (1997b) observed a texture where cordierite appeared to be replaced by sillimanite and biotite and this was interpreted as evidence of a high-temperature retrograde back-reaction with melt remaining in the equilibration volume. Stevens et al. (1997b) concluded from the absence of any post-peak garnet breakdown that retrograde cooling from peak conditions must have been isobaric. These retrograde textural relationships, as well as inclusions of cordierite, sillimanite, quartz and spinel in peak garnets, led Stevens et al. (1997b) to invoke an anticlockwise *P-T* path for the metamorphism. Based on evidence of an ~ 2.02 Ga U-Pb SHRIMP zircon age obtained by Gibson et al. (1997) for a small granite body in the Inlandsee region and evidence for an anticlockwise *P-T* path for the pre-impact metamorphism in the Witwatersrand Supergroup rocks in the collar of the Dome that Gibson and Wallmach (1995) argued was related to the Bushveld Complex event, they attributed this metamorphism to intraplating at deep crustal levels of ultramafic magmas related to the Bushveld Complex at 2.06 Ga. More recently, Perchuk et al. (2002) studied both the collar metapelites and the Steynskraal garnet granulites. Detailed microprobe work from zoned garnet and orthopyroxene led them to propose peak conditions for the M_1 event of around 700 ºC and 5 kbar followed by decompressive cooling to 600 °C and 3 kbar.

Recent geochronological work has yielded an Archaean age of 3.10 - 3.08 Ga for the M_1 event in the core of the Dome (Hart et al., 1999; Armstrong et al., 2006), eliminating the Bushveld Complex as a heat source for the M_1 event. Since the peak event occurred within only 10 – 25 Ma prior to the outpouring of the 3074 ± 6 Ma (Armstrong et al., 1991) Dominion Group lavas, unconformably overlying the Archaean Basement Complex, extremely rapid exhumation rates were invoked by Lana et al. (2006) during D4 extensional unroofing and collapse of the thickened crust. A major problem for these authors was the anti-clockwise *P-T* path with isobaric cooling inferred by Stevens et al. (1997b) for these rocks from petrological evidence. The required rapid exhumation rates could not reconciled with the limited over-thickening of the crust implied by the isobaric cooling P-T path of Stevens et al. (1997b). The incongruence between structural, geochronological and metamorphic models for the Dome, demands a reappraisal of the M_1 metamorphism. In this study, phase equilibria modelling in THERMOCALC is employed to refine estimates of peak conditions and more rigorously constrain fragments of the prograde and retrograde paths based on textural evidence (Chapter 2).

1.4.2 M_2: shock metamorphism (2.02 Ga)

Overprinting the coarse-grained peak assemblage in the Steynskraal granulites from the core of the Dome are shock deformation and other impact-related features formed at 2.02 Ga. These include pseudotachylitic breccias (Reimold and Gibson 2006), recrystallised planar deformation features (PDFs) in quartz (Leroux et al., 1994; Gibson and Reimold, 2005), planar fractures (PFs) in garnet (Gibson and Reimold, 2005), PFs and mosaicism in zircon (Kamo et al, 1996; Gibson et al., 1997), and kink-banding of biotite (Wilshire, 1971; Gibson and Reimold, 2005). Plagioclase exhibits shock-induced planar fractures in the outer parts of the core of the Dome, with isotropisation, PDF development and recrystallisation to microcrystalline, plumose aggregates after diaplectic glass at higher shock pressures toward the centre of the Dome (Gibson and Reimold, 2005). Planar fractures are observed in K-feldspar at low shock pressures in the outer parts of the core of the Dome and recrystallisation after shock melts in the centre of the Dome (Gibson and Reimold, 2005).

Experimental calibrations of shock metamorphic effects in minerals are typically used to determine shock pressure in natural impacts (Chao, 1967; Stoffler, 1972, 1974; Melosh, 1989; Huffman et al., 1993; Langenhorst et al., 1992; Gratz et al., 1992; Huffman et al., 1993, Stoffler and Langenhorst, 1994; Grieve et al., 1996; Fel'dman et al., 2006a, b; Sazonova et al., 2005; Sazonova et al., 2007). Despite kinetic limitations in extrapolating shock behaviour from the scale of experiment to real structures (De Carli, 2002), experimental calibrations have yielded a well-documented and consistent hierarchy of shock effects commonly used to constrain shock pressure distribution on both regional and local scales within impacts. Accordingly, based principally on the observation of PDF occurrence in plagioclase, minimum pressure estimates for the Steynskraal traverse were placed at 15 GPa and maximum pressure estimates of 30 - 35 GPa were proposed based on the evidence for partial to complete isotropisation of feldspar toward the southeast of the traverse (Gibson and Reimold, 2005). These shock estimates are inconsistent with numerical models for the Vredefort structure (Ivanov, 2005), in which minimum shock pressures of 40 GPa are predicted for the Steynskraal traverse. It is conceivable that the marked heterogeneity of shock effects on a thin section and macro-scale (e.g., Gibson and Reimold, 2005) obscure accurate estimates of shock pressure deduced from petrographic studies, and actual shock pressures attained may be much higher, approaching those predicted by numerical models. To test this assertion and more accurately constrain shock distribution across the Steynskraal traverse, an experimental study was undertaken to characterise shock effects in minerals and the extent of shock heterogeneity in a complex polymineralic pelitic granulite analogous to the Steynskraal pelitic granulites as a function of variable shock pressure and pre-shock temperature (Chapter 7). Central to the experimental study is the characterization of progressive structural changes in phases with increasing shock pressure that are typically obscured through annealing in naturally shocked rocks, and which might influence reaction dynamics during corona development associated with post-shock metamorphism.

1.4.3 M_3: post-shock metamorphism (2.02 Ga)

Adiabatic decay of a shock wave following instantaneous, non-adiabatic shock-loading of the crust, leads to residual post-impact heating of the decompressed target material (Raikes and Ahrens, 1979), which may be sufficient to induce static post-shock metamorphism. The post-impact thermal evolution of the Vredefort Dome was modelled using a simple conductive cooling model (Ivanov, 2005). Figure 1.8 demonstrates the cooling history of target rocks at a post-impact depth of 8 km (the estimated present level of erosion – Gibson et al., 1998) and 10 km radius from the centre of the Dome so as to include the Steynskraal traverse. Post-impact temperatures increase slowly within the first hundred thousand years before passing through a thermal maximum attributed to a delayed heating effect of the overlying melt sheet (Ivanov, 2005). For a period of at least 1 Myr, temperatures within 10 km of the core of the Dome are nearly 500 °C higher than the pre-impact temperature of these rocks (440 ± 40 °C for rocks originally buried at 20 - 25 km depth under an 18 °C/km geotherm; Ivanov, 2005). Temperatures for these rocks are predicted to have exceeded the minimum dry solidus of ~800 °C (see Section 6.1 for determination) for 800 Kyr. The presence of an anatectic melt, ubiquitous shock melts and high diffusion coefficients at these temperatures would facilitate diffusion-controlled reaction governed by partial to complete equilibration under the new post-impact conditions.

After the initial thermal maximum was attained 0.2 Myr following impact, the cooling rate from the thermal maximum to the dry solidus exceeded 220 °C/Myr (Figure 1.8). Such rapid cooling rates are unusual, exceeding that of all regional terranes and surpassing the most rapid cooling rates modelled in kilometre-scale contact metamorphic aureoles, e.g., 200 °C/Myr in the Bushveld complex aureole (Johnson et al., 2004; Longridge et al., 2008). Since the Steynskraal traverse occurs within 10 km from the centre of the Dome and solidus temperatures approach 980 °C in the most refractory coronas (Chapter 6), the modelled post-impact temperatures and cooling rates serve as minimum estimates. Actual cooling rates are likely to greatly exceed 220 °C/Myr, within minimum suprasolidus reaction durations approaching 0.2 Myr.

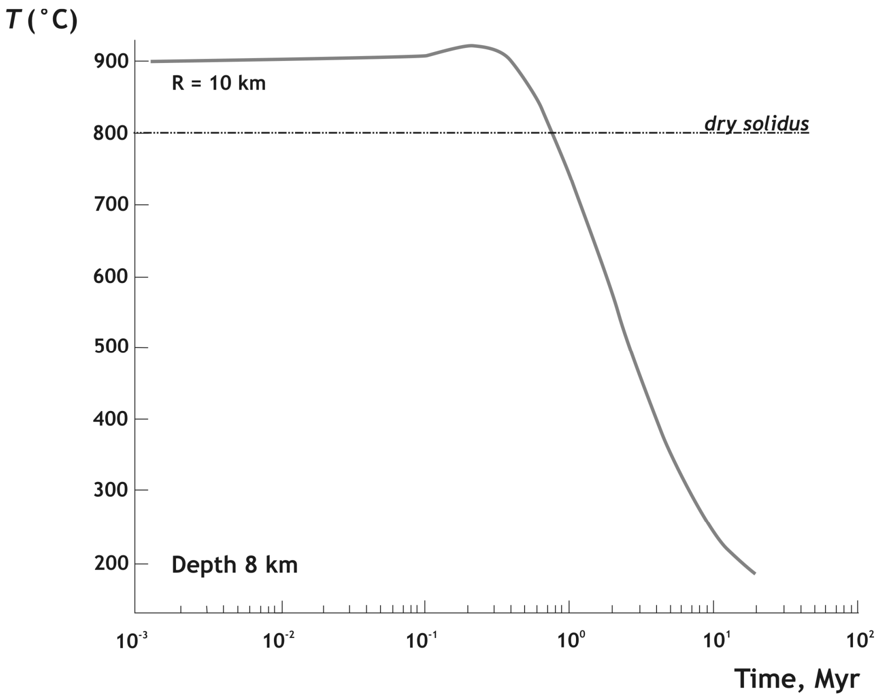

Figure 1.8: Post-impact thermal evolution of target rocks buried at a post-impact depth of 8 km at a radial distance of 10 km from the centre of the Dome (after Ivanov, 2005). Minimum suprasolidus cooling rate from T_{max} is > 220 °C/Myr. The outcrops in the Steynskraal area lie between 5 and 8 km from the centre of the Dome, hence cooling rates are likely to have been even higher.

The immediate application of high temperatures with decay of the shock wave, compounded by the rapid cooling rate (>> 220 °C/Myr) after the thermal maximum is attained, is unique to the Vredefort Dome. Cooling rates are expected to drastically exceed reaction rates, yielding kinetically constrained conditions favourable for preservation of textures developed during the supra-solidus post-impact thermal overprint. The Vredefort Dome, thus, presents the closest-possible natural analogue to laboratory conditions, in which diagnostic textural and compositional intricacies of partial equilibrium are preserved. We are, thus, afforded the opportunity to constrain fundamental reaction mechanisms over a range of temperatures and cooling rates typically obscured in regional terranes because of prolonged reaction rates.

Post-impact heating has manifested in the partial reaction of pre-impact metamorphic assemblages in the Steynskraal granulites, creating distinctive corona textures. Corona textures are developed around garnet and increase in grain size, sectoral complexity and thickness toward the centre of the Dome (Chapter 4 - 6), indicating strong temperature and compositional dependence of the extent of reaction. This makes them ideal for characterizing controls on physico-chemical reaction dynamics during partial equilibration.

Coronas after garnet from the Steynskraal traverse were first investigated in detail by Schreyer and Abraham (1978). They described massive, restitic, garnet granulites characterized by partial to complete replacement of garnet by vermicular orthopyroxene and cordierite symplectite enclosed by a dense rim of orthopyroxene. Microprobe analyses of garnet established homogeneous, almandine-rich compositions despite their corroded nature. Symplectitic cordierite exhibited very narrow compositional variation (X_{Mg}: 0.60 - 0.62; X_{Mg} = Mg/(Mg+Fe)) with low volatile contents. Vermicular orthopyroxene worms in the symplectite were observed to possess higher X_{Al} than the denser rind separating the symplectite from the matrix. Symplectitic orthopyroxene in association with spinel possessed the highest X_{Mg} values. Based on the uniformity of X_{Mg} in orthopyroxene, garnet and cordierite, Schreyer and Abraham (1978) applied the garnet-cordierite thermobarometric calibration of Hensen and Green (1973), which yielded a *P-T* estimate of around 5 kbar and 700 °C. Apparent cross-cutting relationships between pseudotachylitic breccias and garnet pseudomorphs led Schreyer and Abraham (1978) to the conclusion that the peak garnet-bearing assemblage and the coronas formed during a single granulite event related to uplift and exhumation of the Dome. According to them, the pseudotachylitic breccias must, thus, have been emplaced late during the static metamorphism that caused garnet breakdown. This relationship appeared to support a local heat source below the Dome and endogenic models for Dome formation.

Stevens et al. (1997b) described an increase in corona grain size, layer thickness and degree of garnet X_{Mg} zonation toward the centre of the Dome. These workers also conclusively proved that pseudotachylitic breccias pre-dated the symplectite development, based on the occurrence of undeformed symplectite adjacent to and intergrown with the pseudotachylitic breccia assemblage. This evidence, in addition to symplectite-filled shock-induced fractures in garnet, led them to conclude that symplectite formation was intrinsically related to post-impact heating at 2.02 Ga. Thermobarometric estimates using a garnet rim composition in local equilibrium with cordierite and orthopyroxene yielded pressure estimates that ranged between 2.7 ± 0.8 kbar at 700 °C and 3.3 ± 0.13 kbar at 900 °C (Stevens et al., 1997b). Stevens et al. (1997b) were not able to fix temperature directly - the minimum temperature of 680 - 700 °C was based on the presence of the undeformed Central Anatectic Granite (Gibson et al., 1997; Gibson, 2002) in the Inlandsee Pan area some 10 km from the Steynskraal area, and a maximum temperature of 900 °C was based on the maximum stability of biotite and quartz intergrowths in orthopyroxene-bearing granulites at Steynskraal. According to these workers, the pseudotachylitic breccias were generated during impact followed by concomitant annealing of the pseudotachylitic breccia and corona formation. They attributed the absence of corona development between pseudotachylitic breccia and garnet to effective local bulk compositional control, i.e., the matrix composition of the pseudotachylitic breccia (principally comprising feldspar, cordierite and orthopyroxene) is too depleted in silica to allow formation of the diagnostic blocky orthopyroxene-bearing symplectite against garnet, typical of coronas developed between garnet and quartz. This contradicts the apparent cross-cutting relationship between pseudotachylitic breccias and garnet as a temporal constraint of breccia formation relative to corona development proposed by Schreyer and Abraham (1978).

The sectoral complexity, increasing grain size and thickness of coronas toward the centre of the Dome was documented more fully by Gibson (2002). Corona mineralogy was observed to vary sectorally about a relict garnet core depending on the phase originally adjacent to the garnet in the matrix prior to reaction. Spinel in the cordierite-orthopyroxene symplectites was observed to occur in aluminous local effective bulk compositions, i.e., pseudomorphs after sillimanite inclusions in garnet and along silica-deficient fractures in garnet isolated from quartz-rich matrix (Gibson, 2002). Where garnet and quartz were originally juxtaposed, Gibson (2002) observed a cordierite-orthopyroxene symplectite grading into a plagioclase-orthopyroxene symplectite, which in turn is sharply bounded by a blocky orthopyroxene layer (the dense orthopyroxene rim observed by Schreyer and Abraham, (1978)). Elsewhere, where plagioclase initially abutted garnet, Gibson (2002) noted that the blocky orthopyroxene is absent, and a thick cordierite-orthopyroxene symplectite grades outwards into a vermicular intergrowth of biotite, cordierite and plagioclase. Gibson (2002) also observed blocky orthopyroxene around biotite and a biotite-plagioclase symplectite where coarse biotite occurs adjacent to cordierite-orthopyroxene symplectite. Decussate biotite appears to replace both the cordierite-orthopyroxene symplectite and the blocky orthopyroxene, which Gibson (2002) attributed to back-reaction with a melt. K-feldspar moats were observed in close proximity to the coronas, between matrix quartz and plagioclase grains. These potassic moats were interpreted by Gibson (2002) as remnants of a low-proportion partial melt with biotite breakdown under post-impact conditions. The sectoral complexity initially described by Gibson (2002) as a function of local bulk composition is investigated extensively in this study through rigorous petrographic investigation (Chapter 4) and phase equilibria modelling (Chapter 6).

Both Gibson (2002) and Stevens et al. (1997b) noted coarser vermicular orthopyroxene in lower X_{Mg} bulk rock compositions and samples from closer to the centre of the Dome where post-shock temperatures were expected to have been higher. Microanalysis suggested remarkable homogeneity in X_{Mg} for orthopyroxene, but marked difference in X_{Al} depending on textural occurrence (Gibson, 2002). Orthopyroxene in the cordierite-orthopyroxene symplectite is significantly richer in Al than the blocky orthopyroxene rims (0.16 and 0.03 - 0.05 a.p.f.u. respectively; Gibson, 2002). Cordierite X_{Mg} appears to increase inwards toward the garnet rim and within spinel-rich fractures within garnet. Thermobarometry on cordierite-orthopyroxene symplectite pairs in contact with a garnet rim (Gibson, 2002) yielded similar *P-T* conditions to Stevens et al. (1997b). Gibson (2002) attempted to refine post-shock temperatures in the Steynskraal area by applying avPT conventional thermobarometry in THERMOCALC to corona products replacing garnet and biotite. However, temperature estimates were still compromised by large errors (775 ± 50 ºC) (Gibson, 2002) with further refinement required.

Perchuk et al. (2002) identified three generations of orthopyroxene in the Steynskraal metapelites: coarse-grained, Archaean orthopyroxene (Opx_1); blocky orthopyroxene enclosing quartz inclusions in garnet (Opx_2) locally associated with a plagioclase band (Pl_2) toward garnet; and a third generation of symplectitic orthopyroxene (Opx_3). Based on this distinction, they divided the Steynskraal rocks into two groups depending on the presence or absence of coarse-grained orthopyroxene (Opx_1) in the peak assemblage. Group A peak assemblages included Opx_1 in the peak assemblage, whereas Opx_1 was absent from Group B rocks (Perchuk et al., 2002). In their Group A metapelites, Perchuk et al. (2002) described increasing and more variable chemical zonation of Archaean phases, thicker Opx_2 coronas and more irregular compositions of Opx_3 toward the centre of the Dome, which they attributed to stronger ‘impact alteration’. In relatively unaltered Group A metapelites, they noted more aluminous, unzoned compositions of Opx_3 compared to Opx_2 and minor compositional variation in symplectite cordierite (X_{Mg} = 0.77 - 0.79). Orthopyroxene-absent, Group B, metapelites were subdivided into two further subgroups based on the bulk rock X_{Mg} value and degree of ‘impact alteration’. According to Perchuk et al. (2002), Subgroup B1 rocks have higher X_{Mg} values and limited post-impact alteration. Blocky orthopyroxene (Opx_2) has X_{Mg} = 0.42 - 0.44 and symplectitic orthopyroxene (Opx_3) is zoned from X_{Mg} ~ 0.48 to 0.42. X_{Mg} of cordierite decreases from ~ 0.67 to ~ 0.61 from the relict garnet rim towards blocky orthopyroxene. According to them, Subgroup B2 exhibits greater impact alteration and lower X_{Mg} values, with thicker and coarser-grained cordierite-orthopyroxene symplectites and Opx_2 rims (up to 200 µm thick). These workers also observed spinel as inclusions in orthopyroxene (Opx_3) within the cordierite-orthopyroxene symplectite filling fractures cross-cutting garnet. Quartz inclusions in garnet were noted to be almost completely replaced by orthopyroxene (Opx_2). In Subgroup B2, the authors measured marked enrichment in Fe in garnet rims adjacent to cordierite-orthopyroxene symplectite (Perchuk et al., 2002). As for Subgroup B1, X_{Mg} and Al_2O_3 content of Opx_3 and X_{Mg} of cordierite increase toward relict garnet (Perchuk et al., 2002).

Based on their petrographic observations, Perchuk et al. (2002), proposed a peak Archaean metamorphic event followed by two stages of post-impact metamorphism. The Archaean and post-impact trajectories are reproduced in Figure 1.9. A steep decompressive cooling trajectory was obtained for the Archaean event (M_1) from > 700 °C and ~ 5 kbar to 600 °C and ~ 3 kbar at 3074 Ma for the Group A metapelites, by applying thermobarometry to zonation within the coarse-grained phases. The first stage of post-impact metamorphism coincided with formation of blocky orthopyroxene (Opx_2) and adjacent plagioclase (Pl_2) reaction bands in the corona. The compositions of blocky orthopyroxene (Opx_2) and the nearest garnet rim compositions and intervening plagioclase moat (Pl_2), appear to have been used with an unspecified thermobarometric calibration to constrain immediate post-impact conditions. Results are scattered and highly variable with pressure estimates ranging between > 5 kbar and 25 kbar and temperatures between 500 °C and 850 °C. In sample VF5, a decompression-cooling trend was derived using Opx_2, Pl_2 and garnet rim compositions, although it is not explained how the compositions used to derive the path were chosen and how they relate to each other spatially. The second stage of post-impact evolution inferred by Perchuk et al. (2002) entailed the breakdown of garnet to form the cordierite-orthopyroxene (Opx_3) symplectites. In all samples modelled by Perchuk et al. (2002), a subisobaric cooling path was derived from thermobarometry applied to local cordierite-orthopyroxene equilibria, which they assign to unique *P*-*T* conditions sequentially during garnet breakdown, such that cordierite and orthopyroxene with the highest X_{Mg} immediately adjacent to the garnet rim with the highest X_{Fe} were last to form at the lowest temperature. In defining this supposed *P*-*T* trajectory, these authors ignore the Al content of orthopyroxene, regarding Al as 'inert' during corona growth. This is because Al content paradoxically increases toward the garnet rim, suggesting highest temperatures were attained last, an inverse relationship to that inferred by these authors from the Fe and Mg zonation throughout the symplectite.

Perchuk et al. (2002) accommodated the two distinct *P*-*T* trajectories in a three-stage history: According to them, at 3074 Ma, Archaean granulites were exhumed up to the middle crust (3 kbar and 550 °C). This was followed by shock metamorphism at 2023 Ma. Post-impact metamorphism included the formation of pseudotachylitic breccias and rapid heating of the granulites to 750 °C (during which blocky opx and plagioclase corona bands formed), followed by weak decompression to 1 kbar and 550 °C with formation of the cordierite-orthopyroxene symplectites. Post-shock metamorphism is inferred to have taken place over an unspecified long time interval.

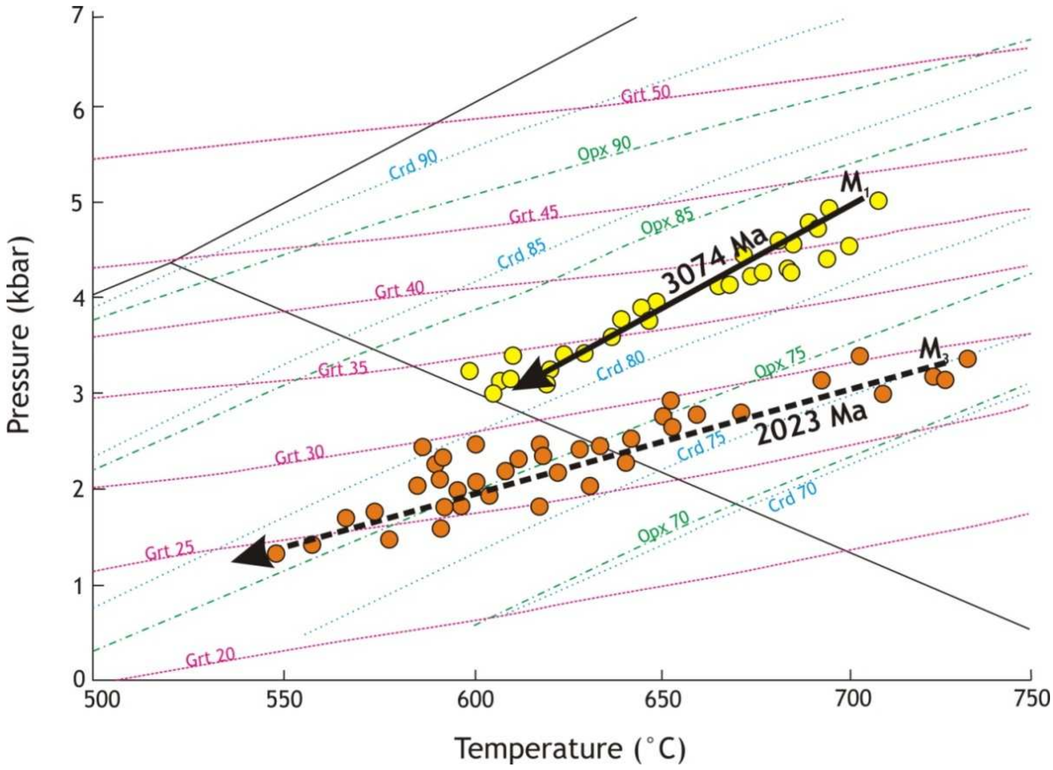

Figure 1.9: Pre- and post-impact P-T trajectories defined by thermobarometry on the cores of peak metamorphic phases and symplectite mineral pairs respectively (reproduced from Perchuk et al., 2002). Yellow circles indicate P-T estimates determined from the core of garnet, orthopyroxene or cordierite Archaean phases and define a decompressive trajectory M_1 (solid black arrow). Orange circles indicate P-T estimates determined from garnet, orthopyroxene and cordierite from the symplectites, defining a P-T trajectory M_2 (dotted arrow).

There are two fundamental problems with the model derived by Perchuk et al. (2002). First, the geodynamic model for Dome ascent prior to impact at 3074 Ma is untenable. These authors require gravitational 'floating' of melt-depleted restites along a shear zone into melt-rich amphibolite facies of lower density. Furthermore, the shear zone invoked is that of the 'Vredefort discontinuity' (Hart et al., 1990), now negated as a terrane boundary, but interpreted as a transition zone from granulite to amphibolite facies by Lana et al. (2003a) and Flowers et al. (2003). The second problem involves a gross underestimation of the duration and scale of processes operating during large impact events. The authors fail to accommodate the immense instantaneous decompression and exhumation of core rocks observed and modelled in large terrestrial impact craters (Ivanov, 2005) in the post-impact *P-T* trajectory. It is also possible that they have erroneously interpreted the zonation in the Archaean phases as a separate event at 3074 Ma, when it is more likely that this zonation developed in response to corona formation. Moreover, it is suspected that Perchuk et al. (2002) used disequilibrium compositions separated by chemical potential gradients to obtain *P-T* estimates in defining *P-T* trajectories. The asymmetrical zonation in Opx_2 composition with respect to Al, Fe and Mg is better explained as a consequence of partitioning of the corona into non-overlapping local compositions owing to variation in limits of intergranular diffusion for these components at constant P and T. In this model of corona formation, variation in X_{Mg} is not related to sequential equilibration of mineral pairs at different pressures and temperatures, although it may be tempting to use mineral pairs at intervals through a structure with asymmetrical zonation to define an apparent decompressive cooling *P-T* trajectory.

1.5 Thesis outline

The previous sections have outlined an unusual polymetamorphic history for the Steynskraal granulites of the Vredefort Dome (Figure 1.10), characterised by equilibrium at a range of scales across the equilibration continuum. A unique opportunity is afforded to constrain intricacies of metamorphism across the equilibration continuum from full equilibration for major components at the metre-scale (M_1) to partial equilibration at the scale of tens to hundreds of microns (M_3) to disequilibrium at all measureable scales (M_2).

A mid- to deep crustal granulite event (M_1) at 3.1 Ga has produced coarse-grained, texturally well-equilibrated restitic assemblages in pelitic and greywacke bulk compositions. New structural models (Lana et al., 2006) and geochronological data (Armstrong et al., 2006) for the Vredefort Dome are inconsistent with an anti-clockwise *P-T* path proposed by Stevens et al. (1997b). In Chapter 2, peak conditions, prograde and retrograde *P-T* paths are reappraised employing more rigorous constraints afforded by phase equilibria modelling in THERMOCALC. M_1 is described as the peak metamorphic event, since it is the main anatectic episode in which the coarse-grained assemblage was produced, even though temperatures were considerably higher in M_2 and M_3.

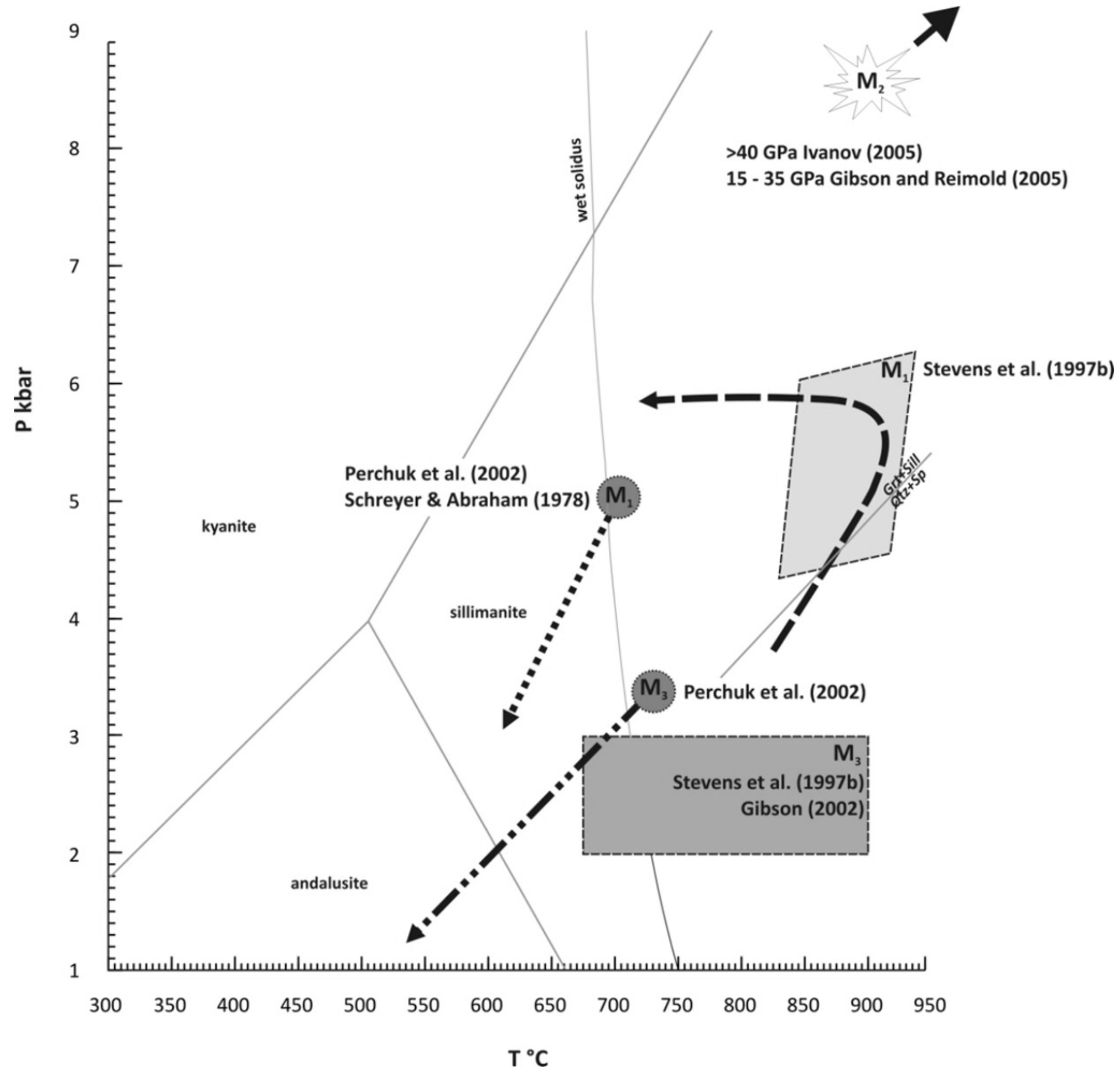

Figure 1.10: P-T diagram demonstrating P-T conditions determined by previous workers for each metamorphic event in the Vredefort Dome.

Post-shock heating with adiabatic decay of the shock wave, following instantaneous non-adiabatic loading of the crust during impact, induced diffusion-controlled corona growth around garnet (M_3). Whilst pressure is reasonably well constrained during corona growth at 2 - 3 kbar (Stevens et al., 1997b; Gibson, 2002; Perchuk et al., 2002), considerable uncertainty still exists regarding the temperature constraints and mechanisms of corona formation during post-impact metamorphism. In this study, the coronas developed after garnet in the Steynskraal granulites are revisited. A comprehensive review of corona formation mechanisms and textures for prograde and retrograde coronas in regional and contact terranes is included in Chapter 3. In

Chapter 4, a detailed petrographic investigation of corona sectoral complexity as a function of bulk rock composition, local domainal composition and distance from the centre of the Dome (i.e., post-shock temperature) is conducted. The Vredefort coronas are compared to the coronas reviewed in Chapter 3 to establish their uniqueness as repositories of information regarding corona formation and equilibration in general. Open-system diffusion metasomatic models of corona formation (Chapter 5) coupled with phase equilibria modelling in THERMOCALC (Chapter 6) are used to constrain the complex interdependency between local domainal bulk composition, post-shock temperature and degree of equilibration, a relationship typically obscured in regional metamorphic rocks owing to prolonged reaction duration. Non-equilibrium thermobarometry is applied to the coronas to more accurately constrain post-impact *P-T* conditions (Chapter 5).

A limitation of the phase equilibria modelling technique employed in Chapter 6 to simulate corona evolution is the inherent assumption that the composition of the effective bulk composition of the corona domain evolves in a linear manner with open-system communication with the surrounding matrix as all components are perfectly mobile throughout reaction history. In reality, the effective bulk composition of the corona domain evolves through a more complex, non-linear open-system interaction with the surrounding rock than accommodated by a simple T-X section. Non-linear compostional exchange between two reactants owing to variable intergranular diffusivities reduces the modal relationships to semi-quantitative at best and yields no information on the spatial organisation of reaction products and evolution of reaction texture. However, given these limitations, T-X sections are able to accommodate higher variance equilibria compared to mu-mu plots and, as such, permit trends in overall modal information preserved in the corona to constrain sources and extents of metasomatic exchange between EBCs. Although mu-mu plots remain the preferred technique with which to model corona textural evolution, there is still valuable information embedded in T-X sections that demonstrates useful relationships so long as the appropriate caution is exercised when interpreting results.

Impact at 2.02 Ga (M_2) has generated highly heterogeneously distributed metastable shock metamorphic effects in minerals indicative of disequilibrium at any scale larger than a few microns. Published estimates of shock pressure distribution throughout the Steynskraal traverse based on observed shock effects in minerals (15 - 35 GPa, Gibson and Reimold, 2005) are in disagreement with predicted shock pressures from numerical models (40 - 45 GPa, Ivanov, 2005). Shock experiments on a pelitic granulite, analogous to the Steynskraal pelitic granulites, are thus undertaken in this study to constrain shock effects in component minerals and shock heterogeneity as a function of shock pressure and pre-shock temperature. This work is one of remarkably few experimental investigations that have been conducted on pelitic polymineralic rocks (Fel'dman et al., 2006a, b; Sazonova et al., 2005). Given an appreciation of the limitations of extrapolating experimental calibrations of shock effects to natural impact structures, this study aims to improve resolution and accuracy of shock pressure distribution across the Steynskraal traverse, through comparison of the experimentally calibrated shock effects in minerals and those observed in reality. Furthermore, an understanding of progressive structural (isotropisation and/or melting) and compositional changes in phases with increasing shock pressure, typically obscured through annealing in naturally shocked rocks, is required when assessing the controls on reaction affinity during corona development associated with post-shock metamorphism.